Ceramics International xxx (xxxx) xxx

Contents lists available at ScienceDirect

Ceramics International

journal homepage: www.elsevier.com/locate/ceramint

Addition of Ag_2O in Er^{3+} doped oxyfluorophosphate glass to allow the drawing of optical fibers

I. Shestopalova [a,*], J. Korri [a], A. Lemiere [a], M. Närhi [a], R. Gumenyuk [a,b], C. Boussard-Plédel [c], J. Troles [c], L. Petit [a,**]

[a] Photonics Laboratory, Tampere University, Korkeakoulunkatu 3, 33720, Tampere, Finland
[b] Tampere Institute for Advanced Study, Tampere University, Kalevantie 4, Tampere, 33100, Finland
[c] Institut des Sciences Chimiques de Rennes (ISCR), University of Rennes 1, UMR 6226, CNRS, F-35000, Rennes, France

ARTICLE INFO

Handling Editor: Dr P. Vincenzini

ABSTRACT

Here, Ag_2O containing glasses in the $NaPO_3$–CaF_2 glass network were prepared using standard melting process. The addition of Ag_2O was found to increase the thermal stability of the glass due to the decrease in the Q^2 units at the expense of Q^1 units, to decrease the intensity of the upconversion under 980 nm pumping and to have a small impact on the nucleation and growth mechanism. Due to the thermal stability against crystallization of the glass prepared with 4 mol % of Ag_2O, we demonstrate that fiber can be drawn from this glass. Despite the formation of Ag nanoparticles at the surface of the fiber although the drawing is a fast process, light can still be confined in the fiber. The fiber exhibits a large emission band centered at 1.5 μm under 980 nm pumping.

1. Introduction

For the past decades, Er^{3+} doped optical fibers have been of great interest as they can be used not only in photonics applications (telecommunications, solar panels, etc.) but also in biomedical applications (bio-imaging, bio-sensing, etc.) [1–4]. Although Er^{3+} doped silica and silicate glasses have been intensively investigated, their main limitation is their low Er^{3+} solubility [5]. Thus, effort has been focused worldwide on the development of new glass compositions with enhanced spectroscopic properties (increased lifetime and larger absorption and emission cross-sections). When developing new glasses to be drawn into optical fibers, it is crucial that the new glasses possess proper thermal properties. Indeed, the glasses should be thermally stable to allow the drawing of optical fiber without crystallizing the amorphous network.

Phosphate glasses are known to have high solubility of rare-earth ions (RE). The luminescence quenching in these glasses occurs at high RE content [6] compared to silica and silicate glasses [6]. As a consequence, when doped with Er^{3+} ions, phosphate glasses are promising as amplifiers and wavelength division multiplexer operating at 1.5 μm [7]. They can also be used as upconversion (UC) lasers (conversion of the IR photons to visible photons) [8], just to cite an example. Recently, the Er^{3+} doped glass with the composition $75NaPO_3$–$25CaF_2$ (in mol%) was reported to be promising, especially for upconversion application. Indeed, intense green and red emissions were observed under NIR pumping after thermally treating the glass to induce the volume precipitation of CaF_2 crystals [9]. However, due to the small temperature difference between the crystallization and glass transition temperatures (~50 °C), fiber can not be drawn from this glass preform. The composition of the phosphate glasses can be easily tailored [10]. However, the change in the glass composition might impact the spectroscopic properties and more importantly the nucleation and growth mechanism as reported recently in Ref. [11]. The thermal stability of the Er^{3+} doped $75NaPO_3$–$25CaF_2$ glass was reported to increase when adding MgO, Al_2O_3 or Fe_2O_3. However, the changes in the glass composition depolymerize the glass network limiting the precipitation of CaF_2 crystals and thus leading to lower intensity of upconversion under NIR pumping compared to the Er^{3+} doped $75NaPO_3$–$25CaF_2$ glass after thermal treatment.

Here, the impact of adding Ag_2O in the Er^{3+} glass with the composition $75NaPO_3$–$25CaF_2$ (in mol%) on the thermal properties is investigated. Ag_2O was selected as it is well known that Ag nanoparticles (NPs) can precipitate during thermal treatment. Due to the surface plasmon resonance (SPR) of Ag NPs, the spectroscopic properties of Er^{3+} doped glass could be enhanced [12,13].

* Corresponding author.
** Corresponding author.
E-mail addresses: iuliia.shestopalova@tuni.fi (I. Shestopalova), laeticia.petit@tuni.fi (L. Petit).

https://doi.org/10.1016/j.ceramint.2023.01.190
Received 19 December 2022; Received in revised form 25 January 2023; Accepted 27 January 2023
Available online 29 January 2023

Table 1
Physical and thermal properties of the investigated glasses.

Glass	T_g (°C) ± 3 °C	T_x (°C) ± 3 °C	T_p (°C) ± 3 °C	$\Delta T = T_x - T_g$ ± 6 °C	ρ (g/cm^{-3}) ± 0.02 g/cm^{-3}
Ag0	296	365	394	69	2.73
Ag0.5	296	361	396	65	2.76
Ag1	297	383	411	86	2.77
Ag2	293	382	413	89	2.82
Ag4	288	383	412	95	2.91

2. Experimental

Phosphate glasses with the composition (in mol%) (98-x) ($0.75NaPO_3 - 0.25CaF_2$) – xAg_2O – $2ErF_3$ with x = 0, 0.5, 1, 2 and 4 (in mol%) were prepared using standard melting quenching technique. The glasses were labeled as Agx. $NaPO_3$ (Alfa Aesar, *tech.*), CaF_2 (Alfa Aesar, *99.5%*), Ag_2SO_4 (Sigma Aldrich, ≥ *99.5%*) and ErF_3 (Alfa Aesar, *99.99%*) were used as the raw materials. The 15g batches were melted in alumina crucible at 1050 °C. After quenching, the glasses were annealed at 40 °C below their respective glass transition temperature (T_g) for 5 h to release the stress from the quench. The 9 cm long preform with 1 cm diameter was prepared from the Ag4 glass and was drawn into fiber with a diameter of ~325 μm using a drawing temperature of 455 °C under helium gas with a flow of 1.5 L/min so the preform is in an inert atmosphere. No coating was used during the drawing to allow the measurement of the thermal and structural properties of the fibers. However, the fibers were fragile and so few meters of fiber were obtained.

Archimedes' method was used to determine the density of the glasses. Densities are given with an accuracy of ±0.02 g/cm^3.

The thermal properties of the glasses were measured using differential thermal analysis (DTA, Netzsch JUPITER F1 instrument). The glass transition temperature (T_g) was taken as the inflection point of the endotherm peak, T_x at the onset of the crystallization peak and the crystallization temperature (T_p) at the maximum of the exothermic peak. The accuracy of measurement is ±3 °C.

The X-ray diffraction (XRD) analyzer Philips X'pert (Philips, Amsterdam, Netherlands) with Cu Kα X-ray radiation (λ = 1.5418 Å) was used to identify the crystalline phases precipitating in the glasses. A "zero-background holder" Fe plate was used as sample holder which was rotated around the Φ-axis at a 16 revolutions per minute. Data were collected with a step size of 0.003°.

A scanning electron microscope (SEM) (Crossbeam 540, Carl Zeiss, Oberkochen, Germany) coupled to an EDS detector (X-MaxN 80, Oxford Instruments, Abingdon-on-Thames, UK) were used to analyze the samples.

The Vis–NIR spectrophotometer (UV-3600 Plus, Shimadzu) was used to measure the absorption and transmittance spectra of the glasses. From the absorption coefficient, the absorption cross-section σ_{abs} (λ) was calculated using Equation (1):

$$\sigma_{abs}(\lambda) = \frac{2.303 \log(I_0/I)}{L \times N_{Er^{3+}}} \quad (1)$$

where log (I_0/I) is the absorbance, L is the thickness of the sample (in cm) and N_{Er}^{3+} is the concentration of rare-earth ions (ions/cm^3). The

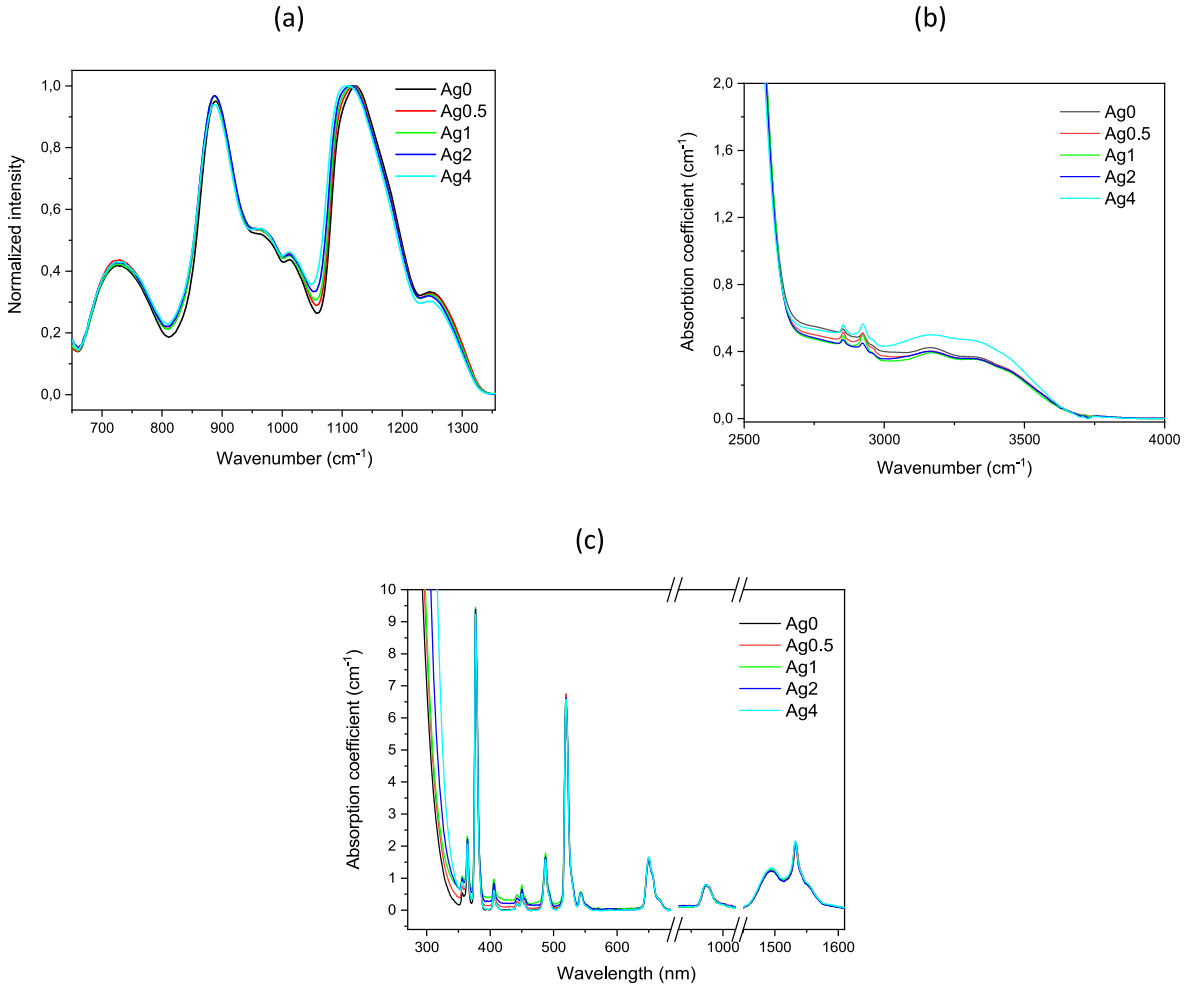

Fig. 1. Normalized FTIR spectra of the glasses (a) and absorption spectra of the glasses in the IR (b) and in the UV–Vis (c) range.

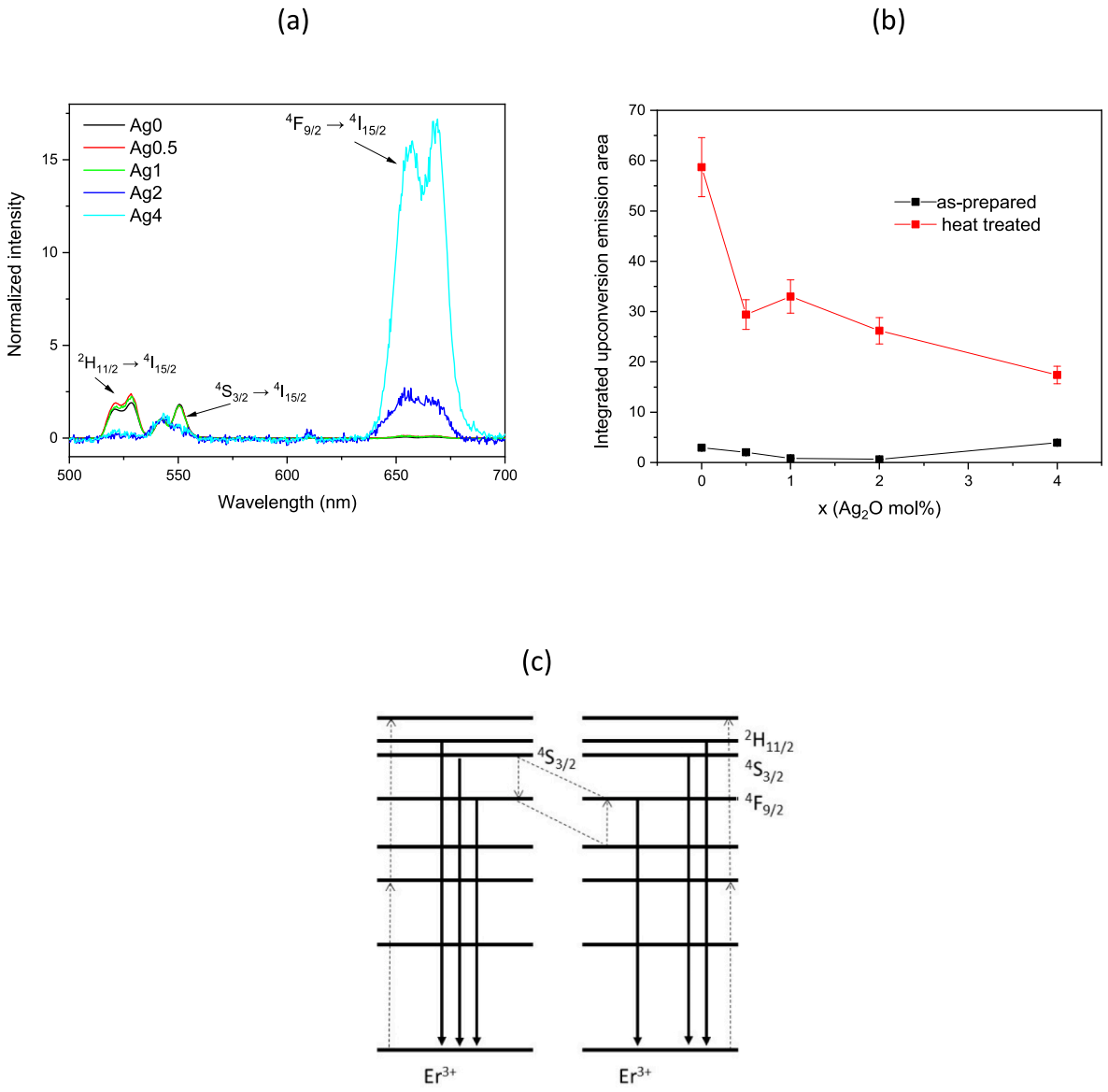

Fig. 2. Normalized upconversion spectra of the glasses (a) and integrated upconversion emission area from 500 to 700 nm prior to (black) and after heat treatment (T_g+20 °C) for 17h and 320 °C for 1h (red) (b) (λ_{exc} = 980 nm). Proposed energy transfer mechanism between Er^{3+} ions (c). (For interpretation of the references to colour in this figure legend, the reader is referred to the Web version of this article.)

accuracy of absorption cross-section is ±10%.

The upconversion (UC) spectra were collected from powder at room temperature using a Spectro 320–131 optical spectrum analyzer (OSA, Instrument Systems Optische Messtechnik GmbH). A continuous-wave 980 nm monochromatic single-mode fiber pigtailed laser diode (CM962UF76P-10R, Oclaro) was used for excitation using 1 A.

The PerkinElmer Spectrum FTIR2000 spectrometer in attenuated total reflectance (ATR) mode was used to measure the IR spectra of the glasses with a resolution of 2 cm^{-1} and 8 scan accumulation.

The spectral transmission and emission of the optical fiber were measured in the 6, 3 or 1.5 cm-long tested fiber samples by launching a broadband light from the fiber-pigtailed white light source (MG922A, Anritsu) or a fiber-pigtailed 980 nm laser source (Coherent), respectively. The white light was used to measure the spectral transmission of the fiber from 600 nm to 1750 nm and the 980 nm laser source was used to measure the emission centered at 1.55 μm. Both light sources were launched into samples by butt-coupling technique via a multimode fiber. The output light was then collected into another multimode fiber and analyzed by an OSA (ANDO AQ6317B).

3. Results and discussion

Er^{3+} doped glasses with the $75NaPO_3$–$25CaF_2$ composition (in mol %) were prepared with different amounts of Ag_2O (x). As depicted in Table 1, an increase in x increases the density, T_x and T_p while it decreases T_g. As a consequence, ΔT, used to evaluate the thermal stability of the glass against crystallization [14], increases when adding Ag_2O in the phosphate glass clearly evidencing that Ag_2O can be used to enhance the thermal stability of the oxyfluorophosphate glass. The Ag1, Ag2 and Ag4 glasses possess a ΔT >90 °C (considering the accuracy of ± 6 °C) suggesting that no crystallization would occur during the fiber drawing from preform. The increase in density with the progressive addition of

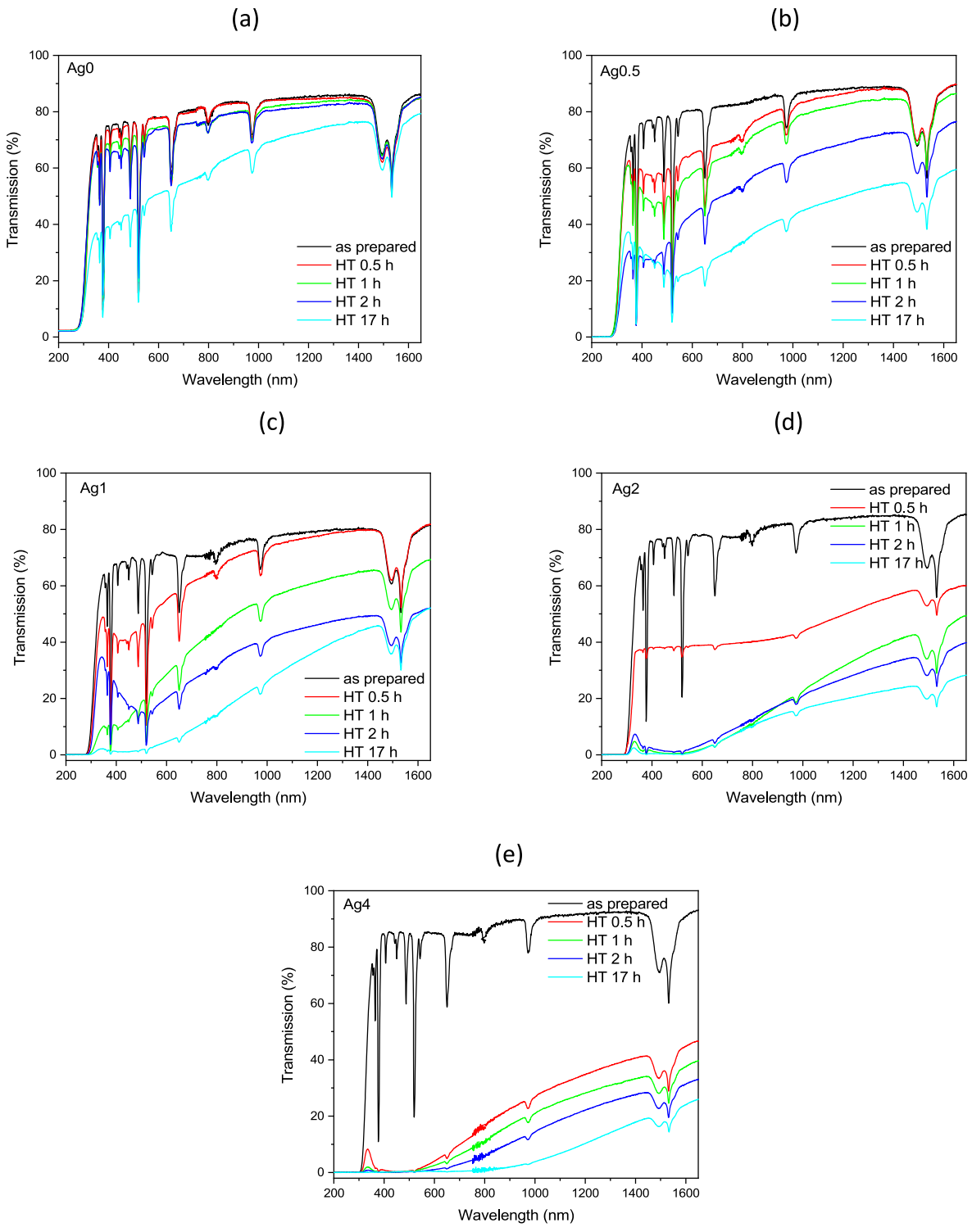

Fig. 3. Transmittance spectra of the investigated glasses with x = 0 (a), 0.5 (b), 1 (c), 2 (d) and 4 (e) prior to and after heat-treatment at (T_g+20 °C) for 30 min to 17h

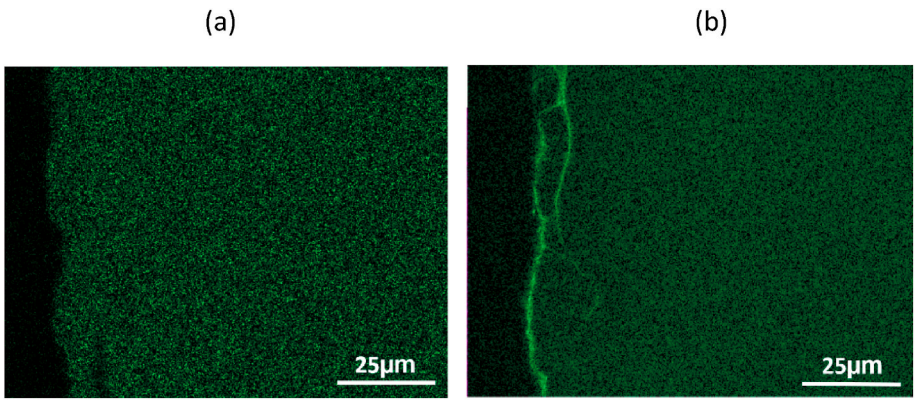

Fig. 4. Ag elemental mapping measured in the cross-section of Ag4 glass prior to (a) and after (b) thermal treatment at (T_g+20 °C) for 17h

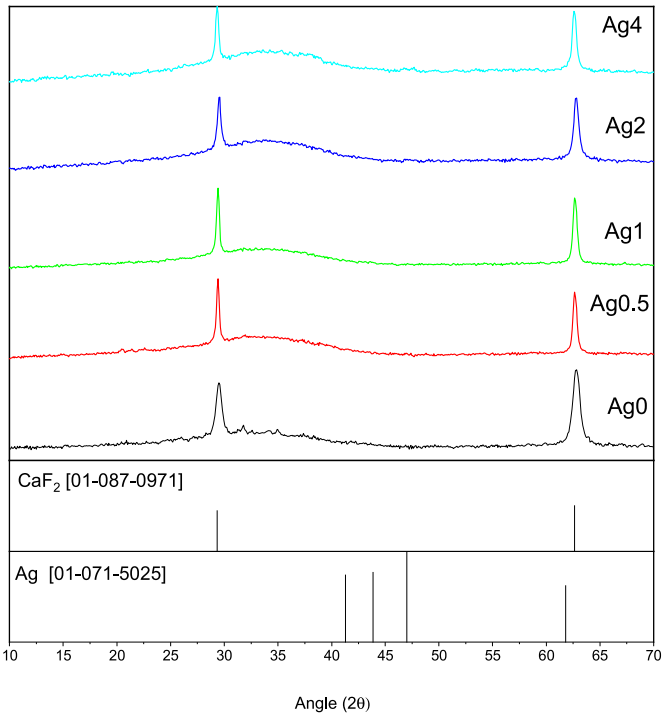

Fig. 5. XRD pattern of the glasses after thermal treatment at (T_g+20 °C) for 17h and 340 °C for 1h

Ag_2O is due to the progressive replacement of $NaPO_3$ and CaF_2 by the heavier Ag.

In order to understand the thermal properties of the Ag containing glasses, the structure of the glasses was investigated using FTIR. As shown in Fig. 1a, the IR spectra are similar to those reported in Refs. [9, 15]. A complete attribution of the IR bands can be found in Refs. [9,15]. The progressive addition of Ag_2O leads to slight changes in the shape of the IR spectrum. An increase in x leads to a slight decrease in intensity of the band at 1250 cm^{-1} compared to the main band, the position of which shifts to lower wavelength. These changes in the IR spectra suggest an increase in the Q^1 units (increase in intensity of the band at ~980 cm^{-1}) at the expense of Q^2 units (decrease in intensity of the band

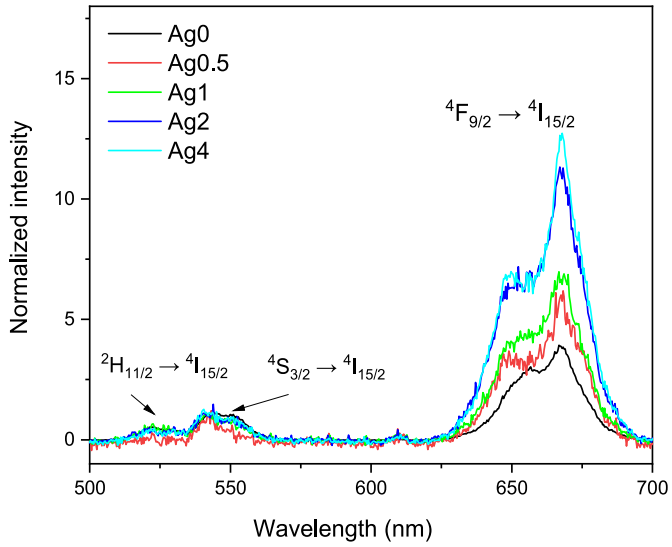

Fig. 7. Normalized upconversion spectra of the glasses after heat treatment at (T_g+20 °C) for 17h and 340 °C for 1h (λ_{exc} = 980 nm).

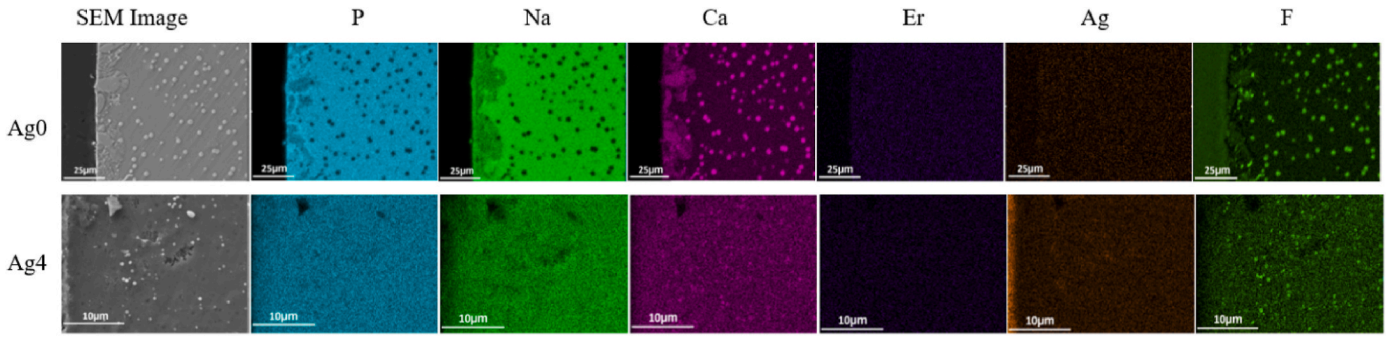

Fig. 6. SEM image of the Ag0 and Ag4 glasses after heat treatment at (Tg+20 °C) for 17h and 340 °C for 1h and mapping of the elements.

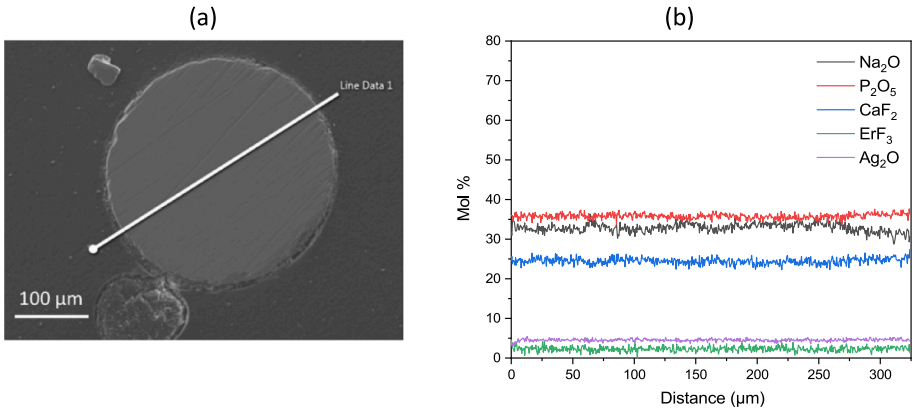

Fig. 8. SEM image of the as-drawn fiber (a) and composition analysis measured across the fiber (b).

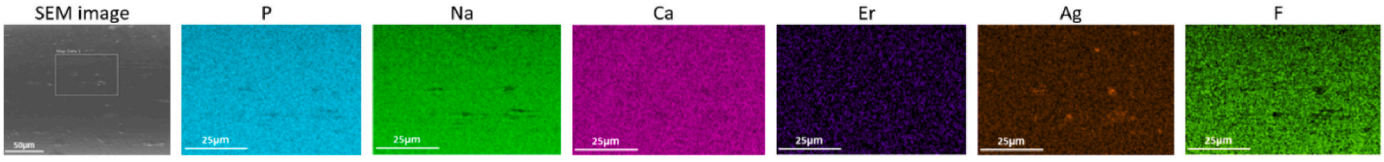

Fig. 9. SEM image of the fiber surface and mapping of the elements.

Table 2
Thermal properties of the preform and the fiber.

	T_g (°C) ± 3 °C	T_x (°C) ± 3 °C	T_p (°C) ± 3 °C	$\Delta T = T_x - T_g$ ± 6 °C
Ag4 preform	288	383	412	95
Ag4 fiber	280	373	409	93

at ~1260 cm^{-1}) when adding Ag_2O in the glass. Therefore, the addition of Ag_2O is thought to depolymerize the phosphate network. Similar changes in the IR spectra were reported when adding other elements such as Al_2O_3, MgO and Fe_2O_3 [11]. The depolymerization of the network is suspected to increase slightly the content of OH groups as evidenced by the increase in intensity of the band located in the 2600–3700 cm^{-1} range, attributed to strongly (2800 cm^{-1}) and weakly (3500 cm^{-1}) associated hydroxyl groups [16] (Fig. 1b).

The changes in the glass structure are also confirmed from the shift of the optical band gap to longer wavelength when x increases (Fig. 1c). The typical absorption bands of Er^{3+} are clearly visible in the absorption spectra of the glasses. They correspond to the transitions from the ground state ($^4I_{15/2}$) to the various excited levels of Er^{3+} ions. Ag^+ cations are expected to be dispersed in the network because of the absence of the SPR absorption band of Ag NPs usually located at ~400 nm [17]. The glasses exhibit similar absorption cross-sections at 980 nm and 1530 nm at (1.6×10^{-21}) and (5.3×10^{-21}) cm^2, independently of their composition. These absorption cross-section values are similar to those reported for phosphate glasses [18]. The shape of the absorption bands remains unchanged after adding Ag_2O in the glass. From the optical properties of the glasses, the site of Er^{3+} ions are suspected to be similar in the investigated glasses.

As shown in Fig. 2a, the addition of Ag_2O in the oxyfluorophosphate network has an impact on the upconversion (UC) properties of the glasses. The UC spectra of the glasses exhibit the typical green (525 and 550 nm) and red (650 nm) emission bands of Er^{3+} ions, which are due to the $^2H_{11/2}$, $^4S_{3/2} \rightarrow {}^4I_{15/2}$ and $^4F_{9/2} \rightarrow {}^4I_{15/2}$ transition of Er^{3+} ions, respectively. According to Ref. [19], the energy-transfer upconversion and excited-state absorption are thought to be responsible for the upconversion luminescence. An increase in x decreases the intensity of the green emission while increasing the intensity of the red emission. It also decreases significantly the integrated upconversion emission area between 500 and 700 nm (Fig. 2b). One should mention that the high overall intensity of emission for the glass with x = 4 (Ag4) compared to the other Ag containing glasses is due to the large intensity of the red emission. The changes in the UC properties when adding Ag_2O in the network suggest modification in the local symmetry of Er^{3+} ions when adding Ag_2O in the glass. However, as the glasses have similar absorption coefficient at 980 nm, the decrease in the intensity of the upconversion can be related to the depolymerization of the phosphate network induced by the addition of Ag_2O and also to the small difference in the content in the OH groups, known as one of the main detrimental factors affecting the upconversion (UC) efficiency [20]. It is also possible that the red emission of Er^{3+} ions is related to a local increase in the concentration of Er^{3+} ions when adding Ag_2O. The high concentration of Er^{3+} is suspected to lead to the $^4S_{3/2} + {}^4I_{9/2} \rightarrow {}^4F_{9/2} + {}^4F_{9/2}$ cross-relaxation between Er^{3+} ions (Fig. 2c) and so to a decrease in the overall emission intensity as suggested in Ref. [21].

A thermal treatment at (T_g+20 °C) for 30 min to 17h was performed in order to check if Ag NPs can grow in these glasses as in Refs. [13,18] during a thermal treatment, such as fiber drawing process for example. The growth of the Ag NPs in the investigated glasses during the thermal treatment was confirmed from the transmittance spectra of the heat treated glasses (Fig. 3). A large absorption band at ~400 nm appears, the intensity of which increases with an increase in x and in the duration of the thermal treatment. This absorption band can be related to the SPR absorption band of Ag NPs [17]. During the thermal treatment, the Ag^+ ions are suspected to change into neutral Ag atoms which aggregate to form Ag NPs. The SPR absorption band shifts to longer wavelength when the duration of the heat treatment increases. These changes in the absorption spectra after the thermal treatment suggest an increase in the number and size of the Ag NPs during the thermal treatment as suggested in Ref. [13]. For long thermal treatment, the SPR bands exhibit a long tail revealing the formation of Ag NPs with non-uniform sizes. One should point out the loss in the transmittance of the glasses after the thermal treatment, especially for the Ag4 glass.

The elemental mapping of Ag obtained using SEM is presented in

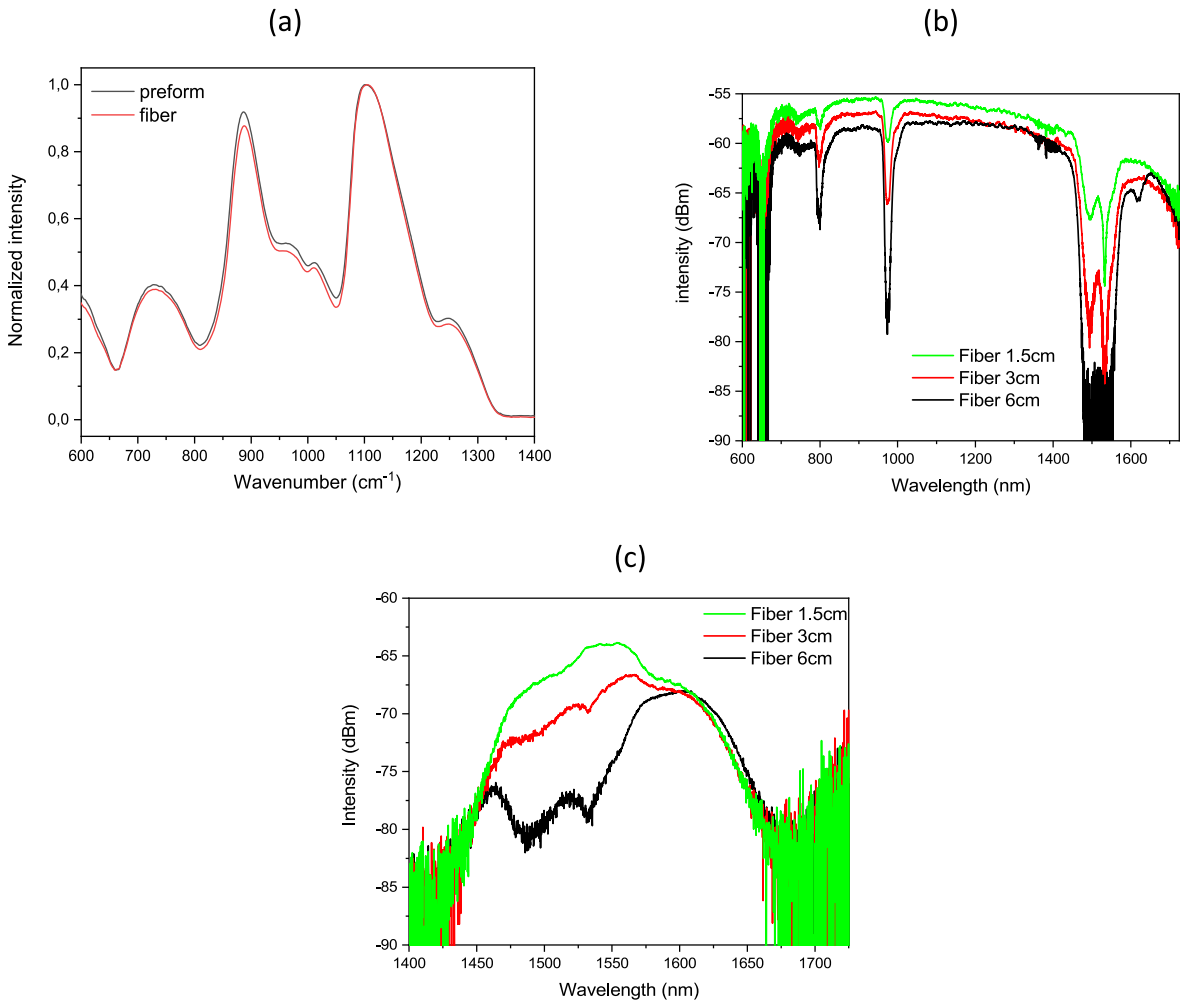

Fig. 10. FTIR (a), Transmittance (b) and Emission (c) spectra (λ_{exc} = 980 nm) of the as-drawn fibers with different lengths. FTIR spectrum of the preform is also shown in (a).

Fig. 4. It clearly shows that Ag species are well dispersed in the as-prepared glass, taken Ag4 as an example (Fig. 4a). After heat treatment, a larger amount of Ag is found at the surface of the glass (Fig. 4b) as in Ref. [18]. No noticeable changes in the shape nor in the intensity of the upconversion bands were observed although enhancement of the UC emission intensities was reported after the Ag NPs formation in tellurite glasses [22]. As the glasses were crushed into powder to allow the comparison of the UC intensities, the layer of Ag NPs is suspected to be too thin even after 17h at (T_g+20 °C) to impact the upconversion properties of the glasses when measured from powder.

The glasses were also heat treated at (T_g+20 °C) for 17h and 340 °C for 1h in order to grow CaF_2 crystals as in Ref. [11] in order to check if the change in the glass composition has an impact on the nucleation and growth mechanism. The XRD pattern of all the heat treated glasses exhibit the peaks related to CaF_2 crystals (Fig. 5). No XRD peaks of Ag could be detected indicating that the amount of Ag nanoparticles in the glasses is too small to be detected.

The volume precipitation of CaF_2 crystals is evidenced in Fig. 6 which shows the SEM and elemental mapping of the cross-section of the Ag0 and Ag4 glasses after heat treatment. Smaller CaF_2 crystals are seen in the heat treated Ag4 glass than in the Ag0 glass.

The precipitation of CaF_2 crystals was also confirmed from the changes in the UC properties of the glasses. The thermal treatment increases the intensity of the upconversion (Fig. 2b). The thermal treatment has also an impact on the shape of the UC spectra. As shown in Fig. 7, the intensity of the red emission is larger than that of the green one after the thermal treatment. These changes in the UC properties of the glasses are again a clear sign of changes in the local symmetry of Er^{3+} ions when the glass network changes from amorphous to crystalline. As suggested in Refs. [11,15], the precipitation of Er^{3+} doped CaF_2 crystals is suspected to lead to cooperative up-conversion process between Er^{3+} ions [23]. However, based on the Er mapping (Fig. 6), some Er^{3+} ions are expected to remain in the glass matrix. The precipitation of CaF_2 crystals is thus thought to lead to cross-relaxation between Er^{3+} ions promoting the red emission of Er^{3+} as discussed in the previous paragraph. However, as depicted in Fig. 2b, the increase in the integrated upconversion emission area from 500 to 700 nm is less as x increases. The depolymerization of the glass network and/or the presence of Ag NPs limits the formation of the CaF_2 crystals limiting the increase in the intensity of the UC emissions. Similar results were reported when adding MgO, Al_2O_3 or Fe_2O_3 in the same glass network [15].

As the addition of Ag_2O in the oxyfluorophosphate glass network increases the thermal stability of the glass, the Ag4 glass was drawn into single core fibers from preform. Uncoated fibers with large diameter were planned to ease the characterization of the crystals if any were found in the fibers and/or at their surface. As the uncoated fibers were brittle, it was not possible to measure the optical losses. Fig. 8 present the SEM image of the fiber and the composition analysis across the fiber. The drawing process has no noticeable impact on the composition of the glass within the accuracy of the measurement (±1.5 mol %) (Fig. 8b).

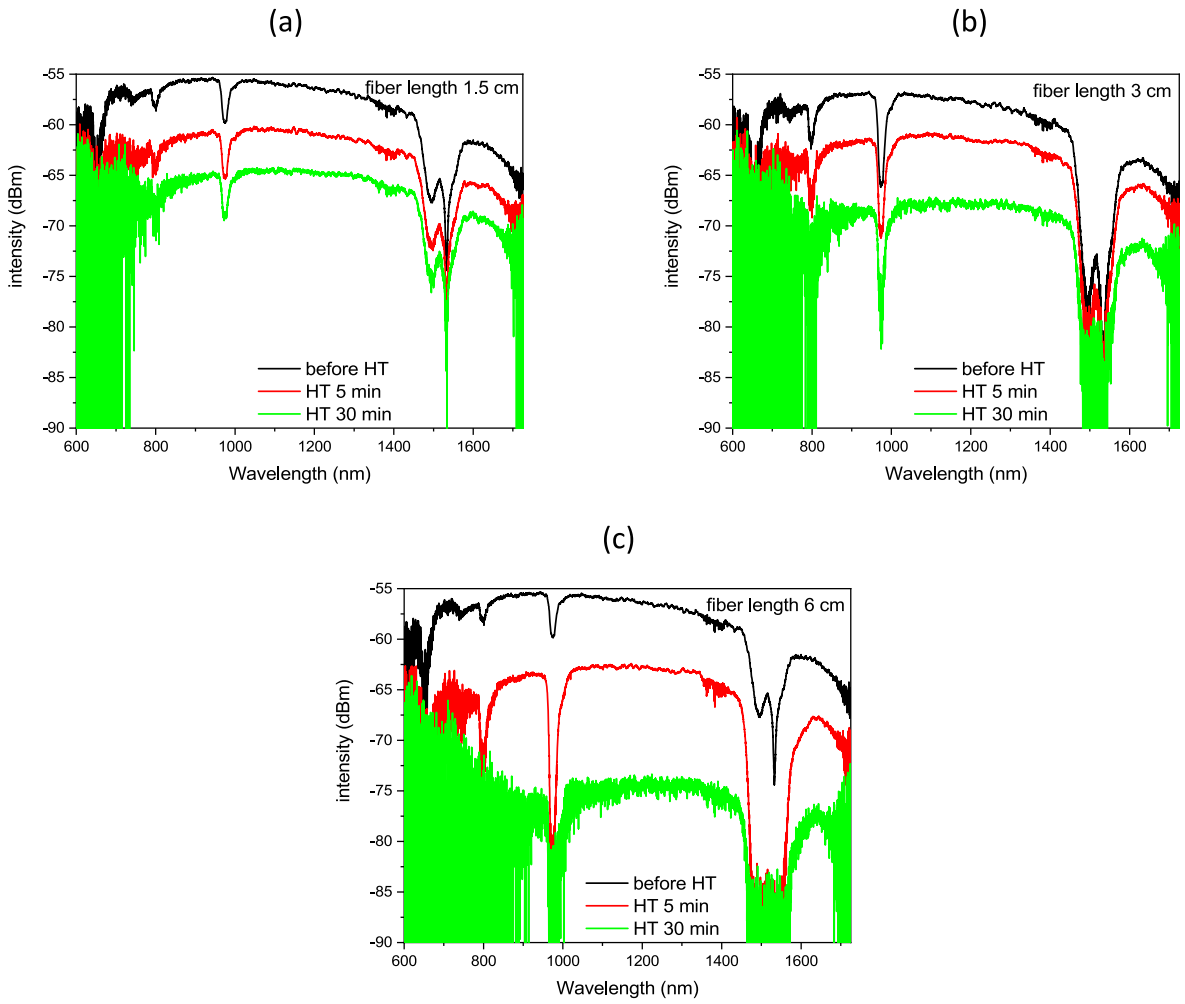

Fig. 11. Transmittance spectra of the fiber prior to and after heat treatment with different lengths: 1.5 cm (a), 3 cm (b) and 6 cm (c).

However, small agglomerates of Ag were found at the surface of the fiber (Fig. 9). One should point out the homogeneous distribution of Na, P, Ca and Er at the surface of the fiber. No crystals were seen in the fiber cross-section (Fig. 8) nor on the surface of the fiber (Fig. 9).

As SEM is not appropriate to quantify F, the thermal and structural properties of the fiber were measured and compared to those of the preform. As shown in Table 2, a slight decrease in T_g and T_x is observed after drawing. This decrease in T_g can be related to the depolymerization of the glass network induced by the drawing process as evidenced by the slight decrease in intensity of the band at 1250 cm^{-1} compared to the main band (Fig. 10a). Similar changes in the thermal and structural properties of phosphate glasses after drawing were reported in Ref. [24]. No sharp peaks can be seen in the IR spectrum of the fiber suggesting that the network remains mainly amorphous during the drawing process as suspected from the SEM analysis.

The transmittance and emission of the as-drawn fibers with three different lengths are presented in Fig. 10b and c, respectively. The transmittance spectrum exhibits the same absorption bands related to Er^{3+} ions as in Fig. 1a. The spectra confirm the confinement of the light in the fibers. The emission spectrum of the 1.5 cm long fiber exhibits the typical emission band of Er^{3+} corresponding to the transition from the excited $^4I_{13/2}$ level to the $^4I_{15/2}$ level of Er^{3+}. However, as the length of the fiber increases, the shape of the emission band changes due to reabsorption of the short wavelengths as reported in Ref. [24].

In order to investigate the possibility to prepare glass-ceramic fiber, the fibers were first heat treated for 5 and 30 min at 300 °C, which corresponds to (T_g+20 °C), as performed on bulks. However, these heat treatments, performed at lower temperature than the temperatures used for the nucleation and growth of CaF_2 crystals, lead to a significant decrease in the transmittance (Fig. 11) and in the intensity of the emission band (Fig. 12). The degradation in the emission properties of the fiber after heat treatment can be related to an increase in the surface roughness due to the formation of a large amount of Ag NPs at the surface of the fiber as depicted in Fig. 13. As shown in Fig. 14, the heat treatment leads also to an inhomogeneous distribution of the elements in the cross-section of the fiber suggesting that crystallization might have occurred during the thermal treatment despite the low temperature used for the thermal treatment. One should mention that, there is no sign of the formation of CaF_2 crystals in the fiber suggesting that the temperature of the heat treatment is probably too low to induce the precipitation of this CaF_2 crystal.

4. Conclusion

As a summary, it was demonstrated that Ag_2O can be used to increase the thermal properties of the Er^{3+} doped glass with the composition $75NaPO_3$–$25CaF_2$ (in mol%) without impacting the volume precipitation of CaF_2 crystals during thermal treatment. Ag nanoparticles were found to precipitate at the surface of the glasses during a thermal treatment performed at temperature near the glass transition temperature.

Although the introduction of Ag_2O leads to the depolymerization of

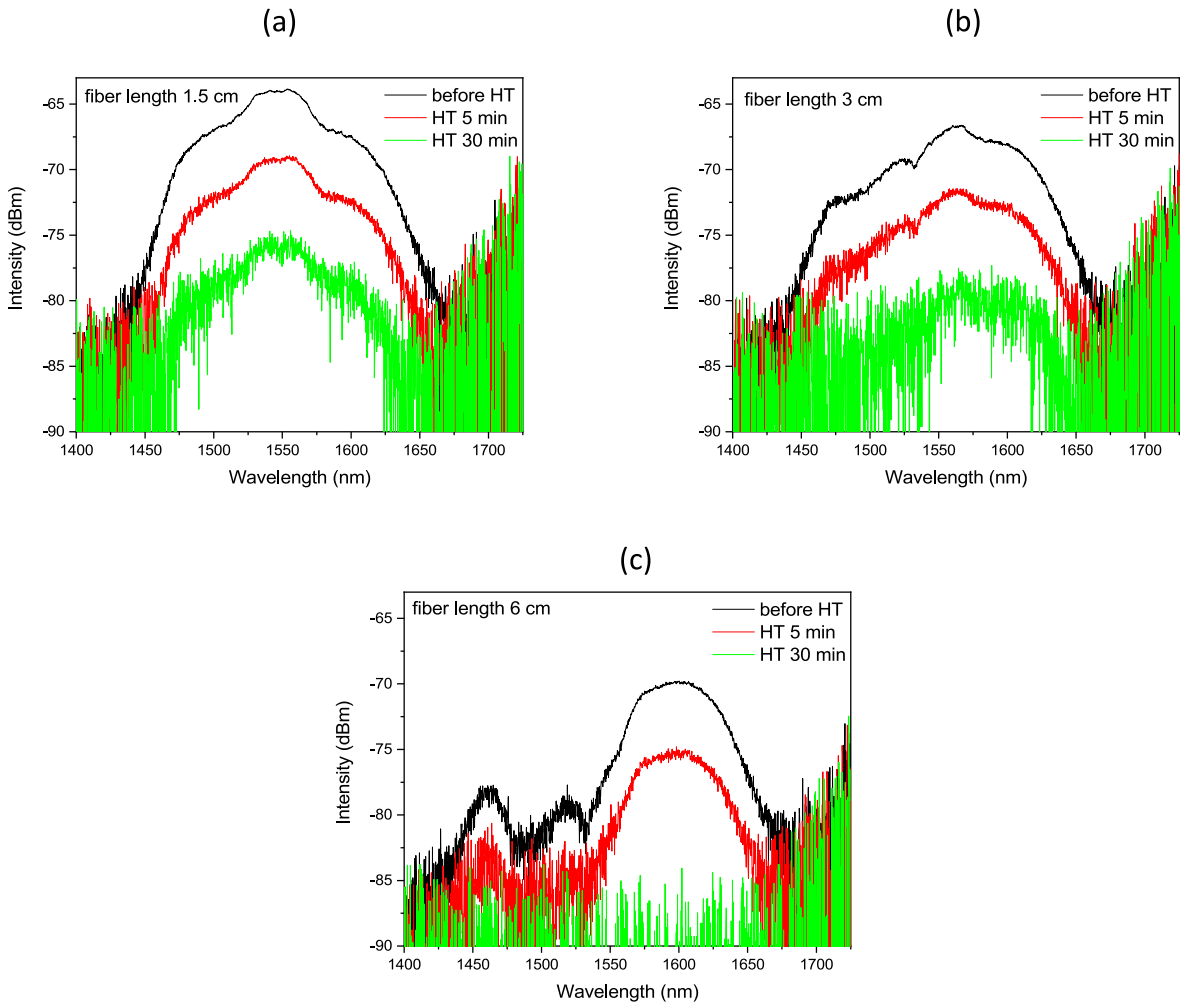

Fig. 12. Emission spectra of the fiber prior to and after heat treatment (λ_{exc} = 980 nm) with different lengths: 1.5 cm (a), 3 cm (b) and 6 cm (c).

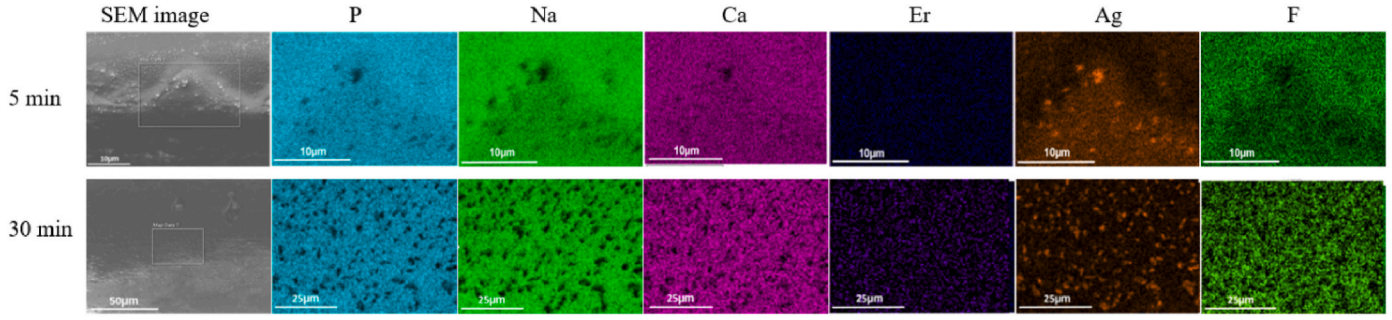

Fig. 13. SEM image of the surface of the fiber heat treated for 5 and 30 min at 300 °C and mapping of the elements.

the phosphate network, the sites of Er^{3+} ions remain unchanged. The addition of Ag_2O in the oxyfluorophosphate network is suspected to limit the precipitation of CaF_2 crystals during thermal treatment. We demonstrate that optical fibers can be drawn from the glass prepared with 4 mol% of Ag_2O without apparent crystallization nor changes in the glass composition. However, Ag nanoparticles form at the surface of the fiber during the drawing although the drawing is a fast process. We also show that this fiber cannot be thermally treated into glass-ceramic fibers due to the formation of additional Ag nanoparticles at the surface of the fiber increasing the optical losses.

Declaration of competing interest

The authors declare that they have no known competing financial interests or personal relationships that could have appeared to influence the work reported in this paper.

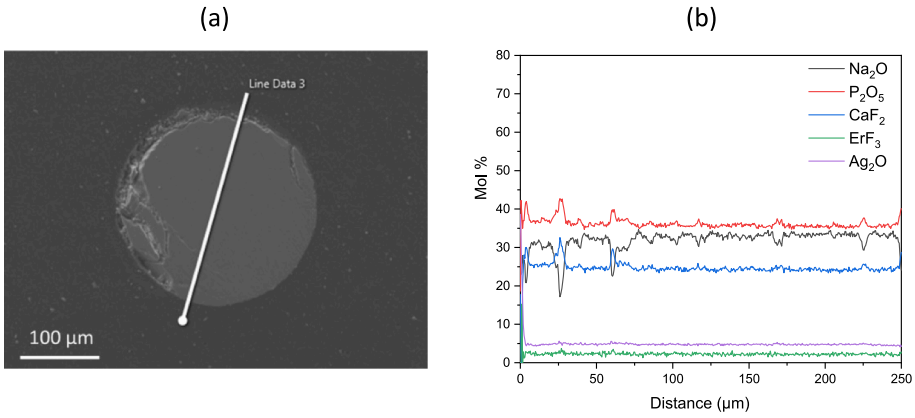

Fig. 14. SEM image of the fiber heat treated for 30 min at 300 °C (a) and composition analysis measured across the fiber (b).

Acknowledgment

Academy of Finland (Flagship Programme, Photonics Research and Innovation PREIN-320165), Pirkanmaa Regional Fund and Magnus Ehrnrooth foundation are greatly acknowledged for the financial support.

References

[1] G. Keiser, F. Xiong, Y. Cui, P.P. Shum, Review of diverse optical fibers used in biomedical research and clinical practice, J. Biomed. Opt. 19 (2014), 080902, https://doi.org/10.1117/1.JBO.19.8.080902.

[2] J. Zhong, D. Chen, Y. Peng, Y. Lu, X. Chen, X. Li, Z. Ji, A review on nanostructured glass ceramics for promising application in optical thermometry, J. Alloys Compd. 763 (2018) 34–48, https://doi.org/10.1016/j.jallcom.2018.05.348.

[3] L. de A. Florêncio, L.A. Gómez-Malagón, B.C. Lima, A.S.L. Gomes, J.A.M. Garcia, L. R.P. Kassab, Efficiency enhancement in solar cells using photon down-conversion in Tb/Yb-doped tellurite glass, Sol. Energy Mater. Sol. Cells 157 (2016) 468–475, https://doi.org/10.1016/j.solmat.2016.07.024.

[4] A. Tünnermann, T. Schreiber, J. Limpert, Fiber lasers and amplifiers: an ultrafast performance evolution, Appl. Opt. 49 (2010) F71, https://doi.org/10.1364/AO.49.000F71.

[5] V.P. Gapontsev, S.M. Matitsin, A.A. Isineev, V.B. Kravchenko, Erbium glass lasers and their applications, Opt Laser. Technol. 14 (1982) 189–196, https://doi.org/10.1016/0030-3992(82)90095-0.

[6] N.G. Boetti, G.C. Scarpignato, J. Lousteau, D. Pugliese, L. Bastard, J.-E. Broquin, D. Milanese, High concentration Yb-Er co-doped phosphate glass for optical fiber amplification, J. Opt. 17 (2015), 065705, https://doi.org/10.1088/2040-8978/17/6/065705.

[7] B.C. Hwang, S. Jiang, T. Luo, J. Watson, S. Honkanen, Y. Hu, F. Smektala, J. Lucas, N. Peyghambarian, Erbium-doped phosphate glass fibre amplifiers with gain per unit length of 2.1 dB/cm, Electron. Lett. 35 (1999) 1007–1009, https://doi.org/10.1049/el:19990668.

[8] L. Feng, L. Bian, J. Nie, H. He, C. Liu, Optical properties and upconversion in rare earth doped oxyfluoride glasses, Optik 169 (2018) 118–124, https://doi.org/10.1016/j.ijleo.2018.05.042.

[9] A. Nommeots-Nomm, N.G. Boetti, T. Salminen, J. Massera, M. Hokka, L. Petit, Luminescence of Er^{3+} doped oxyfluoride phosphate glasses and glass-ceramics, J. Alloys Compd. 751 (2018) 224–230, https://doi.org/10.1016/j.jallcom.2018.04.101.

[10] B.C. Bunker, G.W. Arnold, J.A. Wilder, Phosphate glass dissolution in aqueous solutions, J. Non-Cryst. Solids 64 (1984) 291–316, https://doi.org/10.1016/0022-3093(84)90184-4.

[11] N. Ojha, I. Dmitrieva, W. Blanc, L. Petit, Tailoring the glass composition to increase the thermal stability without impacting the crystallization behavior of oxyfluorophosphate glass, Ceramics 4 (2021) 148–159, https://doi.org/10.3390/ceramics4020013.

[12] H. Fares, H. Elhouichet, B. Gelloz, M. Férid, Silver nanoparticles enhanced luminescence properties of Er^{3+} doped tellurite glasses: effect of heat treatment, J. Appl. Phys. 116 (2014), 123504, https://doi.org/10.1063/1.4896363.

[13] L. Kuusela, A. Veber, N.G. Boetti, L. Petit, Impact of ZnO addition on Er^{3+} near-infrared emission, the formation of Ag nanoparticles, and the crystallization of sodium fluorophosphate glass, Materials 13 (2020) 527, https://doi.org/10.3390/ma13030527.

[14] M. Çelikbilek, A.E. Ersundu, N. Solak, S. Aydin, Investigation on thermal and microstructural characterization of the TeO_2–WO_3 system, J. Alloys Compd. 509 (2011) 5646–5654, https://doi.org/10.1016/j.jallcom.2011.02.109.

[15] N. Ojha, A. Szczodra, N.G. Boetti, J. Massera, L. Petit, Nucleation and growth behavior of Er^{3+} doped oxyfluorophosphate glasses, RSC Adv. 10 (2020) 25703–25716, https://doi.org/10.1039/D0RA04681G.

[16] H. Ohkawa, H. Hayashi, Y. Kondo, Influence of water on non-radiative decay of Yb^{3+}–$^2F_{5/2}$ level in phosphate glass, Opt. Mater. 33 (2010) 128–130, https://doi.org/10.1016/j.optmat.2010.10.027.

[17] P. Gangopadhyay, P. Magudapathy, R. Kesavamoorthy, B.K. Panigrahi, K.G. M. Nair, P.V. Satyam, Growth of silver nanoclusters embedded in soda glass matrix, Chem. Phys. Lett. 388 (2004) 416–421, https://doi.org/10.1016/j.cplett.2004.03.055.

[18] M. Ennouri, L. Petit, H. Elhouichet, Investigations of the thermal, structural, and Near-IR emission properties of Ag containing fluorophosphate glasses and their crystallization process, Opt. Mater. 131 (2022), 112610, https://doi.org/10.1016/j.optmat.2022.112610.

[19] R. Balda, A.J. Garcia-Adeva, J. Fernández, J.M. Fdez-Navarro, Infrared-to-visible upconversion of Er^{3+} ions in GeO_2–PbO–Nb_2O_5 glasses, J. Opt. Soc. Am. B, JOSAB. 21 (2004) 744–752, https://doi.org/10.1364/JOSAB.21.000744.

[20] Y. Feng, Z. Li, Q. Li, J. Yuan, L. Tu, L. Ning, H. Zhang, Internal OH− induced cascade quenching of upconversion luminescence in $NaYF_4$:Yb/Er nanocrystals, Light Sci. Appl. 10 (2021) 105, https://doi.org/10.1038/s41377-021-00550-5.

[21] Q. Ju, X. Chen, F. Ai, D. Peng, X. Lin, W. Kong, P. Shi, G. Zhu, F. Wang, An upconversion nanoprobe operating in the first biological window, J. Mater. Chem. B. 3 (2015) 3548–3555, https://doi.org/10.1039/C5TB00025D.

[22] F. Yang, Q. Zhou, K. Fu, C. Liu, D. Wei, Y. Chen, J. Lu, S. Yang, Upconversion luminescence properties of Er^{3+}-doped TeO_2 –PbF_2 glass with and without Ag nanoparticles, J. Lumin. 156 (2014) 74–79, https://doi.org/10.1016/j.jlumin.2014.07.020.

[23] M.J.F. Digonnet (Ed.), Rare-Earth-Doped Fiber Lasers and Amplifiers, Revised and Expanded, second ed., CRC Press, Boca Raton, 2001 https://doi.org/10.1201/9780203904657.

[24] R. Gumenyuk, A. Poudel, T. Jouan, C. Boussard-Plédel, T. Niemi, L. Petit, Super-luminescence and spectral hole burning effect in ultra-short length Er/Yb-doped phosphate fiber, Opt. Mater. Express 7 (2017) 4358, https://doi.org/10.1364/OME.7.004358.